

Isomer Specific Intercalation Chemistry: Potassium Insertion into the D_2 and D_{2d} Isomers of C_{84}

K. M. Allen,[†] T. J. S. Dennis,[‡] M. J. Rosseinsky,^{*,†} and H. Shinohara[‡]

Contribution from the Inorganic Chemistry Laboratory, Department of Chemistry, University of Oxford, South Parks Road, Oxford, OX1 3QR, U.K., and Department of Chemistry, Nagoya University, Nagoya 464-8602, Japan

Received February 23, 1998

Abstract: Reaction of solids of pure D_{2d} and D_2 C_{84} , as well as mixtures of these isomers, with an excess of potassium produces the cubic phases $K_{8+x}C_{84}$, with multiple occupancy of the octahedral site by potassium. Analysis of X-ray powder diffraction data reveals that the anions adopt well-defined orientations in the solid, driven by the anion–cation contacts. Electron paramagnetic resonance measurements on the solid fullerides indicate that the electronic properties depend on the particular isomer of C_{84} used as host.

Introduction

Since the discovery of superconductivity in K_3C_{60} , the metal intercalation chemistry of the most abundant fullerene, C_{60} , has been extensively developed.^{1–3} There is as yet no consensus on the specific aspects of C_{60} which produce the high superconducting and ferromagnetic transition temperatures in A_3C_{60} ⁴ and (tetrakisdimethylaminoethylene) C_{60} ,⁵ respectively, but the triply degenerate t_{1u} lowest unoccupied molecular orbital (LUMO) and spherical shape may be important chemical features. Studies of reduced derivatives of higher fullerenes have not thus far revealed interesting cooperative electronic properties.^{6,7} The combination of the near-spherical shape and degenerate LUMO of C_{60} is not offered by the ellipsoidal D_{5h} C_{70} molecule. C_{84} occurs predominantly as a 2:1 mixture of the D_2 majority and D_{2d} minority isolated pentagon isomers.^{8,9} D_{2d} symmetry C_{84} is nearly spherical ($r_{\max}/r_{\min} = 1.01^{10}$) and has a doubly degenerate LUMO,¹¹ making it the natural starting point for a detailed investigation into the structural and electronic properties of higher fullerides. The D_{2d} isomer of C_{84} has been isolated in $\eta^2-C_{84}IrCOCl(PPh_3)_2$,¹² but previous studies of the intercalation chemistry of C_{84} have been restricted to photoelectron spec-

troscopy (PES) studies of vacuum-deposited films of the 2:1 mixture of D_2 and D_{2d} isomers of C_{84} . This gave preliminary evidence for a range of phases, but without any indication of metallic behavior.^{13–15}

In this paper we present the results of a study of the intercalation chemistry of the mixed isomer and pure D_2 - and D_{2d} -isomer solids of C_{84} with potassium and report the formation of fcc phases of composition $K_{8+x}C_{84}$ with well-defined orientations of the C_{84} anions and multiple occupancy of the large octahedral site by potassium. This structure forms for either isomer mixtures or the pure isomers, opening the way for the study of isomer-pure phases with partial filling of the degenerate LUMO of C_{84} . Electron paramagnetic resonance (EPR) data on the mixed-isomer solid shows electron localization on discrete, weakly interacting C_{84}^{9-} anions. This may be produced by Franck–Condon barriers to electron transfer between the D_2 and D_{2d} isomers or a Mott–Hubbard gap due to interelectron repulsion. The presence of a much more weakly temperature-dependent component in the susceptibility of $K_{8+x}C_{84}-D_{2d}$ indicates that the electronic properties can depend significantly on the isomer studied.

Experimental Section

C_{76} , C_{78} , and C_{84} were prepared by d.c. arc discharge (300–500 A) of carbon rods ($20^2 \times 500$ mm) in 50 Torr of helium, extraction of the soot with toluene, and repeated HPLC on 5 PYE and Buckyprep (Nacalai $20^2 \times 250$ mm) columns.¹⁶ For C_{84} , this procedure produces a CS_2 -solvated solid which is a 2:1 mixture of the most abundant D_2 (22) and D_{2d} (23) isomers. Solvent was removed by dissolution in benzene, evaporation of the solvent under a flow of N_2 , and application of heat under a dynamic vacuum at 155 °C until a pressure of less than 10^{-5} Torr was attained (typically after 6 h). The first series of intercalation experiments was performed with this isomer mixture as

[†] University of Oxford.

[‡] Nagoya University.

- (1) Rosseinsky, M. J. *J. Mater. Chem.* **1995**, *5*, 1497–1513.
- (2) Prassides, K. *Curr. Opin. Solid State Mater. Sci.* **1997**, *2*, 433–439.
- (3) Fischer, J. E. *J. Phys. Chem. Solids* **1997**, *58*, 1939–1947.
- (4) Hebard, A. F.; Rosseinsky, M. J.; Haddon, R. C.; Murphy, D. W.; Glarum, S. H.; Palstra, T. T. M.; Ramirez, A. P.; Kortan, A. R. *Nature* **1991**, *350*, 600–601.
- (5) Allemand, P. M.; Khemani, K. C.; Koch, A.; Wudl, F.; Holczer, K.; Donovan, S.; Gruner, G.; Thompson, J. D. *Science* **1991**, *253*, 301–303.
- (6) Tanaka, K.; Zakhidov, A. A.; Yoshizawa, K.; Okahara, K.; Yamabe, T.; Kikuchi, K.; Suzuki, S.; Ikemoto, I.; Achiba, Y. *Solid State Commun.* **1993**, *85*, 69–72.
- (7) Zakhidov, A. A.; Yakushi, K.; Imaeda, K.; Inokuchi, H.; Kikuchi, K.; Suzuki, S.; Ikemoto, I.; Achiba, Y. *Mol. Cryst. Liq. Cryst.* **1992**, *216*, 823–830.
- (8) Kikuchi, K.; Nakahara, N.; Wakabayashi, T.; Suzuki, S.; Shiromaru, H.; Miyake, Y.; Saito, K.; Ikemoto, I.; Kainosho, M.; Achiba, Y. *Nature* **1992**, *357*, 142–145.
- (9) Manolopoulos, D. E.; Fowler, P. W.; Taylor, R.; Kroto, H. W.; Walton, D. R. M. *J. Chem. Soc., Faraday Trans.* **1992**, *88*, 3117–3118.
- (10) Saito, S.; Sawada, S.; Hamada, N.; Oshiyama, A. *Mater. Sci. Eng.* **1993**, *B19*, 105–110.
- (11) Nagase, S.; Kobayashi, K. *Chem. Phys. Lett.* **1994**, *231*, 319–324.

(12) Balch, A. L.; Ginwalla, A. S.; Lee, J. W.; Noll, B. C.; Olmstead, M. M. *J. Am. Chem. Soc.* **1994**, *116*, 2227.

(13) Poirier, D. M.; Weaver, J. H.; Kikuchi, K.; Achiba, Y. *Z. Phys. D* **1993**, *26*, 79–83.

(14) Ito, A.; Akaki, O.; Takahashi, T. *J. Electron Spectrosc. Relat. Phenom.* **1996**, *78*, 457–460.

(15) Hino, S.; Matsumoto, K.; Hasegawa, S.; Kamiya, K.; Inokuchi, H.; Morikawa, T.; Takahashi, T.; Seki, K.; Kikuchi, K.; Ikemoto, I.; Achiba, Y. *Chem. Phys. Lett.* **1992**, *190*, 169–173.

(16) Dennis, T. J. S.; Shinohara, H. *Chem. Phys. Lett.* **1997**, *278*, 107.

Table 1. Reaction Conditions for the Preparation of the Isomer-Pure and Mixed Isomer Samples of K_xC_{84} Phases Studied Here

conditions	mixed isomers	D_{2d} isomer	D_2 isomer
initial reaction with potassium at 250 °C in days	3.5	2.5	3.5
annealing:			
ramp rate to 250 °C/deg min ⁻¹	1.0	1.4	2
period at 250 °C/h	6	1	0.5
ramp rate to 300 °C/deg min ⁻¹	0.5	0.5	1
period at 300 °C/h	12	4	2
ramp rate to 350 °C/deg min ⁻¹	0.25	0.25	0.5
period at 350 °C/h	48	48	29

the host solid. The second series of intercalation reactions was carried out with pure samples of the D_2 and D_{2d} isomers prepared by an adaptation of the original separation procedure.¹⁷

The intercalation procedures used for all three fullerenes were similar, so the procedure for C_{84} is detailed here. The C_{84} host solid (1–3 mg, 1–3 μ mol) was loaded into a Pyrex insert and taken into a drybox where it was loaded into a larger diameter Pyrex tube together with a 100-fold excess of potassium metal contained in a 3 mm diameter glass capillary. The reaction vessel was evacuated to 10^{-4} Torr and sealed and then placed into a furnace with a mean temperature of 250 °C and a gradient of 5–8 °C between the hot end containing the C_{84} host powder and the cooler end where the potassium metal condensed. The vessel was heated under these conditions for 4 days. The product was then removed in the drybox and resealed in a Pyrex tube for isothermal annealing for 2 days at 350 °C. The precise heating conditions for the three samples of C_{84} studied are given in Table 1. The samples were then sealed under helium in 0.5 mm diameter capillaries for X-ray diffraction and EPR measurements. The X-ray powder diffraction data were recorded at station 9.1 of the Daresbury Laboratory Synchrotron Radiation Source with an X-ray wavelength of 1.00 Å (calibrated with an Si standard) over the angular range $3^\circ \leq 2\theta \leq 40^\circ$ for 8 h with a step size of 0.05°. Data were analyzed with the Rietveld method using the GSAS¹⁸ and PROFIL¹⁹ programs. A pseudo-Voigt peak shape function and a 36-term Chebyshev polynomial background function were employed in the GSAS refinements. EPR data were collected using a Varian E-line spectrometer at a microwave frequency of 9.23 GHz between 5 and 300 K; g values were calibrated with a DPPH standard, and the magnetic susceptibility was calibrated using K_3C_{60} , whose susceptibility was taken to be 8.5×10^{-4} emu mol⁻¹.²⁰ The power dependence of the EPR signals was checked in all cases at 5 K to avoid saturation of any of the signals reported. The powers used were 0.05 and 0.004 mW, for $K_{8.39}C_{84}-D_{2d}$ and $K_{7.91}C_{84}-D_2$, respectively.

Results

X-ray Powder Diffraction. The X-ray patterns of the products of reaction of both C_{76} and C_{78} with excess potassium were indicative of the formation of an amorphous solid, displaying a broad maximum without any discernible Bragg reflections. In contrast, the equilibration of the C_{84} isomer mixture with potassium vapor produces an X-ray powder diffraction pattern which indicates cubic metric symmetry and systematic absences consistent with face-centering. Le Bail extraction²¹ in space group $Fm\bar{3}m$ gives a lattice parameter $a = 16.592$ Å. Refinement of the structure involved a two-stage procedure, initially concentrating on the cation positions and

then taking the orientational order of the C_{84}^{n-} anions into account. Preliminary structural analysis was performed with recognition that the isomer mixture would make an early attempt to assign anion orientational order difficult. Rietveld analysis was therefore carried out with the PROFIL program¹⁹ in which the scattering density from the C_{84} anions was approximated as a spherical shell of charge with refinable radius R ($f(C_{84}) = [84/\sqrt{(4\pi)}]f_c \sin(QR)/QR$, where Q is the momentum transfer and $f(C_{84})$ and f_c are the spherical shell C_{84} and carbon atom form factors at Q). Adequate simulation of the intensities at high angles was not possible from this approach, but reflections with d spacings of less than 2 Å ($2\theta < 22^\circ$) were sufficiently insensitive to the fulleride orientational order to allow the location of the intercalated cations to be probed. The retention of fcc packing in the potassium-saturated phase suggests that the large octahedral interstitial site is multiply occupied, by analogy with the fcc $Na_{6+x}C_{60}$ phases.^{22,23} The potassium cations occupy xxx positions at the corners of a cube produced by displacement away from the center of the octahedral site parallel to the $\langle 111 \rangle$ directions. The most satisfactory agreement was obtained by 64(3)% occupation of the tetrahedral site, 28-(3)% occupancy of the center of the octahedral site, and 85-(1)% occupation of the xxx cube corner positions. The refined value of the spherical shell radius of 4.17(2) Å is physically reasonable.¹⁰ The refined composition was $K_{8.5(2)}C_{84}$, and the problems with the fit apparent to the {622}, {444}, and {551} reflections could be alleviated by increasing the potassium concentration to 10.3(2) by the occupation of other positions within the large octahedral site, notably a “square antiprismatic” site produced by rotation of the top face of the K_8 cube by 45° about the [001] direction. Subsequent investigations on the isomer-pure fullerides indicated that the improvement to the refinement was spurious; these cation positions are not actually occupied but refine when the spherical shell model is used by accounting for missing scattering density due to neglect of the C_{84} anion orientational order. Any attempt to locate the cations precisely must deal with the anion orientations.

The reactions with the pure samples of the D_2 and D_{2d} isomers also produced diffraction patterns which can be indexed as fcc; the lattice parameters are reported in Table 2. The data on the D_{2d} isomer is of higher quality than the D_2 -derived phase, and so we choose to concentrate on the description of the refinement of this data set. Initial refinements with the spherical shell model were adequate at low angle (though again requiring inclusion of the “square antiprism” potassium positions) but were clearly insufficient to fit the high angle data. The D_{2d} molecular symmetry is lower than the $m\bar{3}m$ (O_h) point symmetry of the site occupied in the crystal by the C_{84} anion, and therefore orientational disorder is inevitable, although this does not necessarily equate with spherical disorder. Partial orientational order may be achieved by alignment of the $\bar{4}$ axis of the molecule with the cube axes: there are then two possible orientation choices. The normals to the mirror planes cutting through the 6:6 bonds can be aligned with the $\langle 100 \rangle$ directions ($\bar{4}m2$ symmetry) or along the $\langle 110 \rangle$ face diagonals ($42m$ symmetry), as shown in Figure 1. (In the D_2 case the orientation is defined by the molecular 2-fold axes.) Both of the above discrete orientations gave much better fits than the spherical shell model but the $42m$ symmetry had considerably

(17) Dennis, T. J. S.; Kai, T.; Tomiyama, T.; Shinohara, H. *Chem. Commun.* **1998**, 619.

(18) Larson, A. C.; von Dreele, R. B. *General Structure Analysis System*; Los Alamos National Laboratory, 1994.

(19) Cockcroft, J. K. *Program PROFIL*; Birkbeck College, London **1997**.
 (20) Wong, W. H.; Hanson, M. E.; Clark, W. G.; Gruner, G.; Thompson, J. D.; Whetten, R. L.; Huang, S.-M.; Kaner, R. B.; Diederich, F.; Petit, P.; Andre, J.-J.; Holczer, K. *Europhys. Lett.* **1992**, *18*, 79–84.

(21) LeBail, A.; Duroy, H.; Fourquet, J. L. *Mater. Res. Bull.* **1988**, *23*, 447–452.

(22) Rosseinsky, M. J.; Murphy, D. W.; Fleming, R. M.; Tycko, R.; Ramirez, A. P.; Siegrist, T.; Dabbagh, G.; Barrett, S. E. *Nature* **1992**, *356*, 416–418.

(23) Yildirim, T.; Zhou, O.; Fischer, J. E.; Bykovetz, N.; Strongin, R. A.; Cichy, M. A.; Smith, A. B., III; Lin, C. L.; Jelinek, R. *Nature* **1992**, *360*, 568–571.

Table 2. Refined Parameters for $K_{8+x}C_{84}$ Prepared from D_{2d} , D_2 , and Isomer-Mixture C_{84} Hosts^a

	D_{2d}	D_2	isomer mixture
R_{wp}	0.0151	0.0113	0.0182
R_{exp}	0.008	0.0068	0.0049
χ^2	3.82	2.92	14.44
χ^2 for incorrect orientation	6.76	3.97	31.1
R_{wp} for Le Bail extraction in $Fm\bar{3}m$	0.0148	0.0106	0.0163
wavelength/Å	1.00011	1.00068	1.00066
lattice parameter/Å	16.536(6)	16.561(7)	16.559(5)
C $U_{iso}/\text{Å}^2$	0.07(2)	0.090	0.032(8)
K x	0.233(2)	0.237(4)	0.231(2)
tetrahedral occupancy	0.221(7)	0.219(8)	0.222(5)
xxx $U_{iso}/\text{Å}^2$	0.01(2)	0.05(2)	0.03(1)
K x	0.3902(4)	0.3923(4)	0.3884(3)
cubic cluster occupancy	0.79(1)	0.743(12)	0.842(9)
xxx $U_{iso}/\text{Å}^2$	-0.022(6)	-0.043(7)	0.007(5)
K x	0.5	0.5	0.5
octahedral occupancy	0.30(3)	0.21(3)	0.35(2)
xxx $U_{iso}/\text{Å}^2$	0.11(5)	0.1	0.18(5)
overall stoichiometry	8.39(17)	7.91(19)	8.86(11)

^a The carbon temperature factors were fixed in the D_2 case; in this refinement the parameters quoted arise from the competitive refinement of the $\langle 100 \rangle$ and $\langle 110 \rangle$ orientations of the 2-fold symmetry axes of the molecule, as described in the text. The total concentration of tetrahedral potassium is four times the quoted occupancy, due to the disordered displacement away from the center of the tetrahedral site.

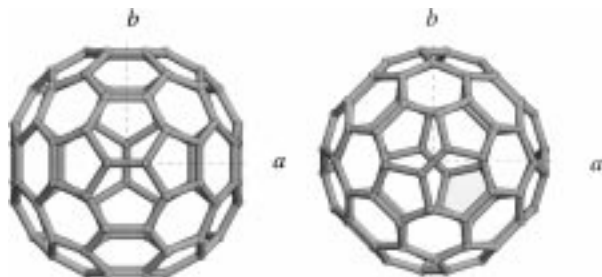


Figure 1. The two possible orientations of the D_{2d} isomer of C_{84} in an fcc unit cell, viewed along the unique 4 axis of the molecule: (i) mirror plane normals directed along $\langle 100 \rangle$ and (ii) mirror plane normals directed along $\langle 110 \rangle$. Orientation (ii) is indicated strongly by Rietveld refinement for the D_{2d} isomer in the isomer-pure solid and for both the D_2 and D_{2d} isomers in the mixed-isomer phase. The experimental data is less definitive in the D_2 case (orientations shown in Supporting Information), with competitive refinement indicating 68% of the $\langle 110 \rangle$ orientation.

superior agreement indices ($\chi^2 = 3.8$ vs 6.76 for $\bar{4}m2$, $R_{F^{**2}} = 2.1$ vs 5.5%) and an essentially perfect agreement at high angles, indicating that the anion orientations are correctly determined. Competitive refinement of the two orientations gives less than 1% of the $\bar{4}m2$ orientation. The relevant Rietveld refinements are presented in Figure 2.

The adoption of tetragonal space group symmetry would allow the $\bar{4}2m$ orientation to be completely ordered throughout the solid, whereas the cubic symmetry found actually produces additional 6-fold orientational disorder due to the absence of a 3-fold axis in the C_{84} molecule. Refinements in which the anions were perfectly orientationally ordered in space groups $I\bar{4}m2$ (formed by a 45° rotation of the fcc cell vectors to produce the familiar $a/\sqrt{2} \times a/\sqrt{2} \times a$ body-centered tetragonal (bct) representation²⁴ of the fcc cell; thus the $\bar{4}2m$ orientation in fcc is equivalent to $\bar{4}m2$ in bct) and $P\bar{4}n2$ (giving the anions at the

origin and body center of the cell orientations differing by 90° rotation about $[001]$) gave similar, but not improved, agreement with the c/a ratio remaining close to the fcc value of $\sqrt{2}$. This indicates that the Bragg reflections from the present samples are too broad to allow effective distinction between the possible small tetragonal distortion induced by perfect orientational order and the fcc cell discussed in the remainder of the paper, although the orientations adopted by the anions can be unambiguously described. The occurrence of long-range orientational disorder of a locally well-ordered molecular orientation has precedence in the ‘‘Stephens model’’ for $Fm\bar{3}m$ symmetry K_3C_{60} .^{25,26} The derived parameters and agreement indices are given in Table 2. The maximum peak height in the final difference Fourier map is less than 0.5% of the maximum in the F_{obs} map.

The inclusion of the correct anion orientation in the Rietveld refinement allowed a stable and convincing refinement of the locations of the potassium cations. The tetrahedral site is 89-(2)% occupied. The center of the octahedral site is 30(3)% full while the cube corner positions of the K_8 group situated around the octahedral site center are 79(1)% occupied, giving a refined composition of $K_{8.39(17)}C_{84}$. The K–K distances in the multiply occupied octahedral site are given in Table 3 for all three samples. The positions of the eleven carbon atoms in the asymmetric unit of the D_{2d} isomer of C_{84} could not be refined, but their isotropic displacement parameters were refined together to a value of 0.07 Å^2 . The structural model was sufficiently stable to allow separate refinement of displacement parameters for the three independent potassium positions. The tetrahedral site refined to a value larger than that conventional in the now-familiar C_{60} fullerides of 0.09 Å^2 . Disordered displacement of this cation away from the center of the tetrahedral site along a 3-fold axis onto an xxx position improved the fit slightly and reduced the temperature factor. The parameters from refinement of this model are quoted in Table 2. The temperature factor of the octahedral potassium refined to 0.09 Å^2 . This is larger than values for the other sites, consistent with refinements on other fullerides.^{25,26} Omission of this potassium or significant reduction in the site occupancy severely degrades the quality of the fit, particularly to the $\{311\}$ and $\{440\}$ reflections, with a 10% increase in R_{wp} to 1.63%. The displacement parameters of the cube corner cations refined to a smaller value.

Partial orientational order of the majority D_2 isomer is also possible in cubic symmetry. Alignment of one of the 2-fold axes with the $\langle 100 \rangle$ directions allows two distinct 222 symmetry orientations related by 45° rotation, in which the remaining two 2-fold axes are aligned with either the $\langle 100 \rangle$ or $\langle 110 \rangle$ directions, producing a similar orientation choice to the D_{2d} case. While either orientation gave a superior refinement to the spherical shell, the lower crystallinity of the isomer-pure D_2 compound did not allow such a detailed elucidation of the anion orientational order. It was clear that the anions were not ordered solely along $\langle 100 \rangle$ ($\chi^2 = 3.97$), but a clear distinction could not be drawn between 50% of each orientation ($\chi^2 = 3.02$) and 100% of the $\langle 110 \rangle$ orientation ($\chi^2 = 2.97$). Competitive refinement gave 68% of the D_2 molecules aligned in the $\langle 110 \rangle$ orientation ($\chi^2 = 2.95$). The potassium cations occupy the same positions found in the D_{2d} case, refining to a composition of $K_{7.91(19)}C_{84}-D_2$.

For the mixed-isomer host, the data indicated similar crystallinity to the D_{2d} compound and refinement indicated a high proportion of both isomers of the fullerene anions adopting the

(24) Fleming, R. M.; Rosseinsky, M. J.; Murphy, D. W.; Ramirez, A. P.; Haddon, R. C.; Siegrist, T.; Tycko, R.; Dabbagh, G.; Hampton, C. *Nature* **1991**, 352, 701–703.

(25) Stephens, P. W.; Mihaly, L.; Lee, P. L.; Whetten, R. L.; Huang, S.-M.; Kaner, R.; Diederich, F.; Holczer, K. *Nature* **1991**, 351, 632–634.

(26) Allen, K. M.; David, W. I. F.; Fox, J. M.; Ibberson, R. M.; Rosseinsky, M. J. *Chem. Mater.* **1995**, 7, 764–770.

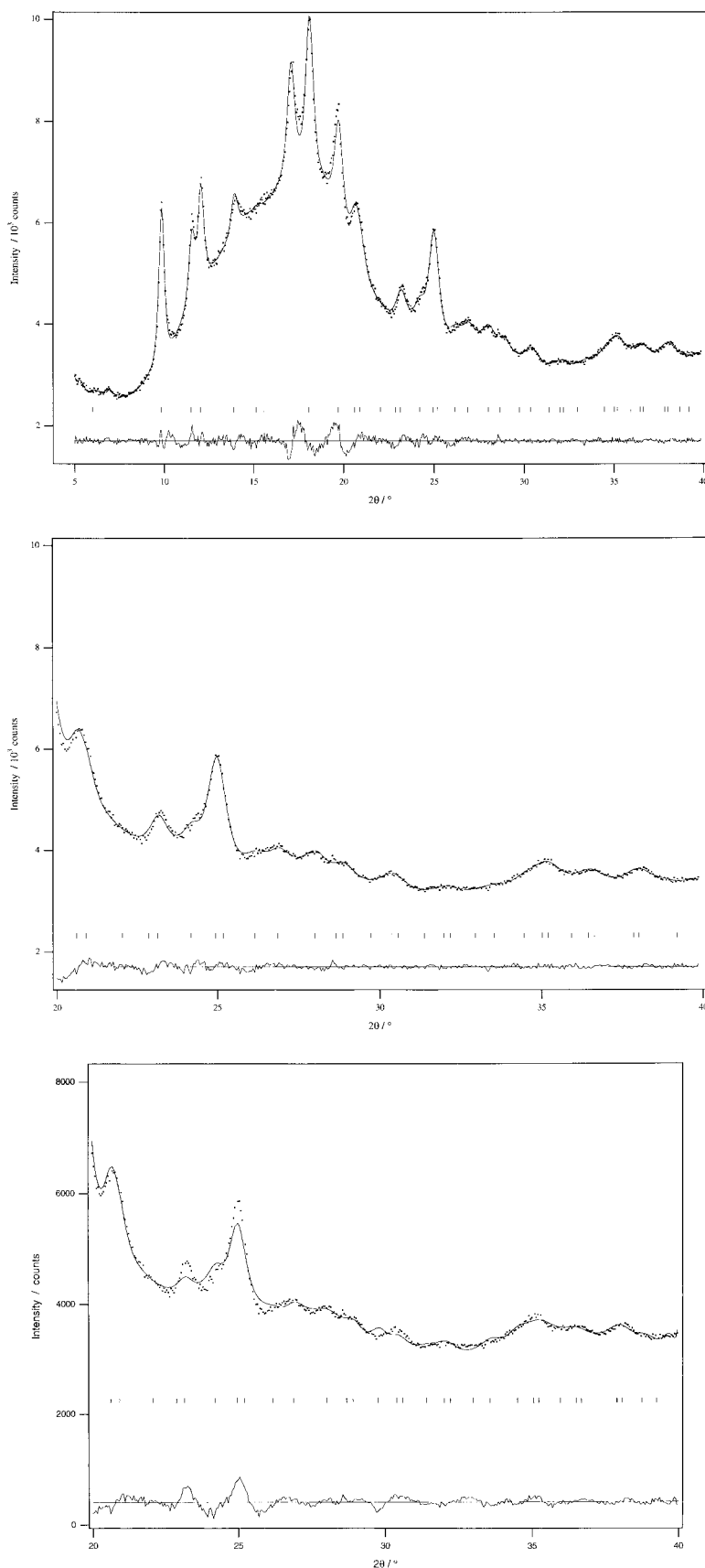


Figure 2. Rietveld refinement of synchrotron powder X-ray diffraction data collected on $K_{8.39(17)}C_{84}-D_{2d}$ on station 9.1 of the SRS at Daresbury Laboratory. Ticks mark the positions of the Bragg reflections. The observed data are shown as points, the calculated fit is a solid line, and the difference curve is marked below. (i) Full angular range, with the refinement model having anions in the $\langle 110 \rangle$ orientation. (ii) Data for $20^\circ \leq 2\theta \leq 40^\circ$ for the model with the anions in the $\langle 110 \rangle$ orientation. (iii) Data for $20^\circ \leq 2\theta \leq 40^\circ$ for the model with the anions in the $\langle 100 \rangle$ orientation. The degradation in fit quality in (iii) is apparent. The broad maximum in the scattering between 10° and 24° comes from the capillary used to contain the sample.

Table 3. Distances (Å) within the K_{8+x} Unit Refined on the Octahedral Site of the Three $K_{8+x}C_{84}$ Phases Studied Here^a

distance within K_8 cube	D_{2d}	D_2	mixed host
cube edge	3.631(2)	3.566(2)	3.697(1)
face diagonal	5.135(3)	5.043(3)	5.228(2)
center–corner	3.145(2)	3.088(1)	3.202(1)

^a The center–corner distance is from the octahedral site center to the xxx position at the cube corner and is not required in interpretation of the average structure, as discussed in the text.

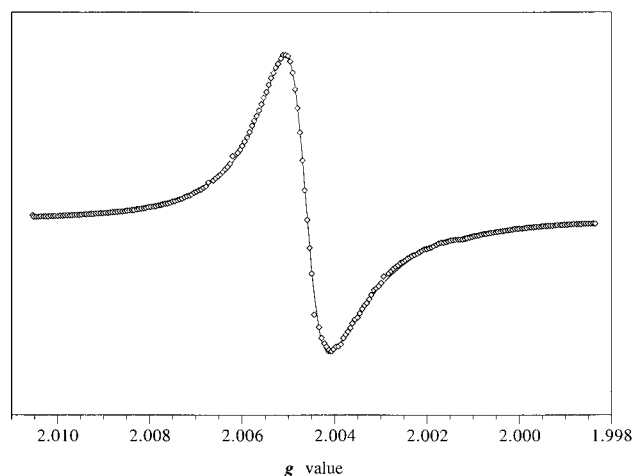
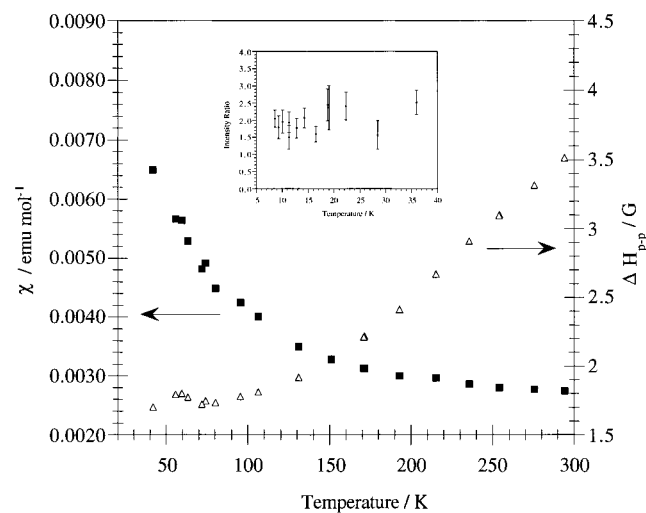


Figure 3. (i) Variation of the EPR-derived susceptibility (filled squares) and peak-to-peak line width (empty triangles) of mixed-isomer $K_{8.86(11)}C_{84}$. The inset shows the ratio of the intensity of the two signals resolved below 40 K. (ii) Fit to the 8 K EPR signal of mixed isomer $K_{8.86(11)}C_{84}$ with two Lorentzian line shapes.

$\langle 110 \rangle$ orientation. Competitive refinement of fullerene orientations after optimization of all other parameters indicated that all the D_{2d} anions and 96% of the D_2 anions were oriented along $\langle 110 \rangle$, as found for $K_{8+x}C_{84}-D_{2d}$. The mixed isomer phase refined to give the highest potassium concentration of $K_{8.86(11)}C_{84}$.

EPR Spectroscopy. (a) K_xC_{76} , K_xC_{78} . Insertion of potassium is demonstrated by the single Lorentzian EPR signal found for both samples, with pure Curie behavior for $4 \text{ K} \leq T \leq 300 \text{ K}$ corresponding to 15% (4%) $S = 1/2$ spins and line widths of between 4.2 (1.4) to 6.2 (2.5) G for K_xC_{76} (K_xC_{78}).

(b) $K_{8.86(11)}C_{84}$ Mixed Isomer. The temperature-dependence of the EPR-derived susceptibility and peak-to-peak line width (ΔH_{pp}) of the mixed-isomer solid $K_{8.86(11)}C_{84}$ are shown in Figure 3(i). The spectrum at 300 K can be fitted with a single derivative Lorentzian line. Calibration of the absolute intensity

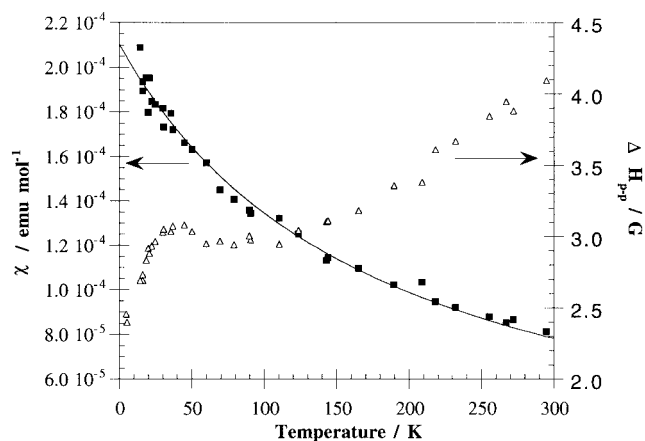


Figure 4. The majority EPR signal ($g = 2.0019(3)$) from $K_{8.39(17)}C_{84}-D_{2d}$ (presented as in Figure 3i) shows a much less pronounced temperature dependence of the susceptibility, χ_{EPR} , than those found for the other two C_{84} host solids.

of the EPR signal allows the fitting of a Curie–Weiss law to the temperature-dependent intensity, revealing that there is approximately one unpaired spin for every C_{84} molecule, consistent with the 86(11)% $S = 1/2 C_{84}^{9-}$ anions expected from the refined composition and providing confirmatory evidence for it. The spectra below 40 K cannot be at all satisfactorily fit as a single Lorentzian signal; two Lorentzians in an intensity ratio of approximately 2:1 are required. The fit to the EPR signal at 8 K is given in Figure 3ii, and the inset to Figure 3i shows the variation of the ratio of the two signals with temperature. This strongly suggests that the EPR spectra at low temperature can be interpreted as arising from the two $S = 1/2 C_{84}^{9-}$ anions from the D_2 and D_{2d} isomers. The two signals have $g = 2.00044(14)$ (D_2) and $g = 2.00047(14)$ (D_{2d}).

(c) $K_{7.91(19)}C_{84}-D_2$. EPR measurements on the single isomer $K_{7.91(19)}C_{84}-D_2$ display two Lorentzian signals which exhibit localized electron behavior at all temperatures, with weak interanion interactions indicated by the Weiss constant of -2 K . The more intense signal strongly resembles in both line width and position the more intense signal from the mixed-isomer sample. The signal has reduced absolute intensity in this isomer-pure case, corresponding to only 0.30(5) unpaired spins per fullerene molecule. This reduced value is consistent with the reduced amount of potassium intercalated into the $C_{84}-D_2$ host. The $C_{84}^{8-}-D_2$ anion is expected to be diamagnetic, and the quantitative disagreement between the refined composition and the number of free spins is within the errors of both EPR and refined determinations of the number of $S = 1/2$ 7–anions expected.

(d) $K_{8.39(17)}C_{84}-D_{2d}$. The EPR data for the phase prepared from the isomer-pure D_{2d} host show two Lorentzian signals at all temperatures, corresponding to a total spin count of 0.45 per anion, in reasonable agreement with the C_{84}^{9-} radical anion concentration expected from the refined composition. The dominant signal at low temperatures strongly resembles (in peakwidth but not in g value) the less intense signal present in the mixed-isomer data, corresponding to 0.13 unpaired electrons per fullerene. More interesting is the behavior of the second signal which is shown in Figure 4. This signal is qualitatively different from those observed for the mixed-isomer or D_2 -isomer-pure fullerenes. At temperatures above 15 K its intensity can be well fitted by a Curie–Weiss law with a magnitude corresponding to 0.32(4) electrons per fullerene anion. However, the large Curie temperature of -182 K indicates that the strict Curie law interpretation is unphysical. Below 50 K, both the

line width and g value depart from a smooth temperature dependence, while the intensity increases sharply below 15 K, adding to the evidence that this signal does not arise solely from isolated impurity spins.

Discussion

The shape of higher fullerenes appears critical in the generation of crystalline fullerides, with the near-spherical C_{84} yielding crystalline products in contrast to those of the C_{76} and C_{78} molecules. This can be ascribed to the lower symmetry of the nonspherical C_{76} and C_{78} compared with C_{84} . The crystal structure of $K_{8+x}C_{84}$ is of considerable interest; the obvious difference with C_{60} is that the “saturated” phase formed by reaction with excess potassium has fcc rather than bcc symmetry and displays multiple occupancy of the octahedral site. An fcc K_9C_{70} phase has been observed,²⁷ suggesting that the change in interstitial site size as the fullerene size increases is important in controlling the crystal chemistry.

The lattice parameters for the three fcc phases derived from the different hosts are similar, but that for the isomer-pure $K_xC_{84-D_{2d}}$ is smaller than those for the D_2 and mixed isomer (67% D_2) compounds, suggesting that the more spherical D_{2d} molecules can pack together more efficiently. In all the hosts, the larger lattice parameter when compared with C_{60} naturally increases the sizes of the interstitial sites, which may be calculated from the refined spherical shell radius of C_{84} as $r_{\text{octahedral}} = 2.43$ (1.70) Å and $r_{\text{tetrahedral}} = 1.33$ (1.00) Å (the values for fcc C_{60} are given in parentheses). The size match with potassium for the tetrahedral site appears particularly favorable. The slight increase in displacement parameter of the fully occupied tetrahedral site over the C_{60} case^{25,26,28} may be a reflection of the larger interstitial sites in C_{84} , producing disordered displacement of the tetrahedral cation along the $\langle 111 \rangle$ directions.

The orientational ordering of the anions is only partial but is significant as may clearly be seen by noting the inadequacy of the fit using only a spherical shell to model the scattering density from the C_{84} . The $42m$ (D_{2d}) and 222 (D_2) symmetries of the C_{84} isomers might suggest a tendency to crystallize in tetragonal and orthorhombic space groups, respectively. The cubic symmetry observed implies either partial or total orientational disorder as neither molecule has a 3-fold axis, with partial order clearly demonstrated by refinement. The unique axis in a tetragonally oriented structure in the D_{2d} case would be defined by alignment of the molecular $\bar{4}$ axis (which passes through the midpoint of a 6:6 bond, Figure 1) along the c direction. In the observed cubic symmetry, occupation of this direction by the other two orthogonal 2-fold axes produces the 3-fold orientational disorder, doubled by the mirror planes with their normals perpendicular to cell vectors.

The preference for partial over total orientational disorder may be ascribed to the avoidance of over-close contacts between the potassium cation on the tetrahedral site and the carbon atoms. The molecular point symmetry of the two C_{84} isomers has important consequences for the details of the orientational order. The orientation of the 6:6 bond aligned perpendicular to the cell vectors is rotated by 45° from that found for the C_{60}^{3-} anion in fcc K_3C_{60} .²⁵ The reason for both the existence and the precise type of anion orientational order can be understood by considering the environment around the tetrahedral sites. The potassium

cations are large enough to cause the fulleride anions to “nest” into each other to increase the effective size of the tetrahedral hole, as has been found in K_3C_{60} ,²⁵ despite the enlarged interstitial site sizes with the C_{84} host. The K–C distance should be at least 3.08 Å, the sum of the van der Waals radius for C and the ionic radius for K^+ . As there are too few observables to refine the anion structure, the following discussion treats the fulleride anion as a rigid unit. The distances from the tetrahedral site to the adjacent C atoms in the D_{2d} case (with the observed $\langle 110 \rangle$ anion orientation) range from 3.29 to 3.63 Å while in the D_2 case the contacts lie between 3.18 and 3.69 Å. The mean distance is 3.48 Å for both isomers, suggesting that the same factors are responsible for the observed anion orientations in each case. For a statically or dynamically spherically disordered fulleride anion, the distance from the tetrahedral site to the carbon shell is only 3.01 Å, apparently too close to allow free fulleride rotation or static orientational disorder of the fullerene molecules.

In addition to suppressing spherical disorder, the tetrahedral potassium cations select the alignment of the D_{2d} molecules with their mirror planes oriented normal to the $\langle 110 \rangle$ directions, rather than the $\langle 100 \rangle$ directions. When the $\langle 110 \rangle$ orientation is adopted, the tetrahedral potassium cation is located directly over the centroids of four six-membered rings from the neighboring C_{84} anions. Figure 5 shows the view along two of the four vectors from the tetrahedral site to these neighbors for orientationally ordered fullerene molecules in the $I4m2$ space group. In the case where the molecular mirror planes are oriented along the $\langle 100 \rangle$ direction (space group $I42m$), however, this favorable arrangement around the tetrahedral cation is lost. Instead, the cation is located off-center from the four neighboring hexagonal rings, as illustrated by the view along the $[021]$ direction shown in Figure 5(iii). The K–C distances would be as close as 3.03 Å (tetrahedral potassium) and 2.70 Å (cube corner potassium).

Because the D_{2d} and D_2 molecules are topologically so similar (the D_{2d} molecule corresponding to splitting the D_2 molecule in half and rotating one-half with respect to the other by 90°) and in $Fm\bar{3}m$ there are C_4 axes passing through the lattice points, the two fullerenes have similar carbon positions once disordered, and so similar $K\cdots C$ distances are found for the D_2 isomer. The $\langle 110 \rangle$ orientation is also favored by refinement on the mixed-isomer $K_{8.86(11)}C_{84}$, containing 67% of the D_2 isomer, showing that the D_2 and D_{2d} molecules both adopt the same $\langle 110 \rangle$ orientation and suggesting that the cation–anion interactions determine the observed orientational order for both isomers.

The D_2 and D_{2d} point symmetry of the two C_{84} isomers explains why the quality of fit is similar in both the orientationally ordered $I4m2$ and $P4n2$ and orientationally disordered $Fm\bar{3}m$ models. In $Fm\bar{3}m$ there are C_3 axes along the cube diagonals (the viewing vectors in Figure 5). The orientationally ordered molecules have a hexagon centroid located along each of these directions. This is not a C_3 axis of the C_{84} molecule itself, because this hexagon is surrounded by two pentagons and four hexagons, (unlike the more symmetrical C_{60} in which it is a true C_3 axis), but can be seen as a “pseudo- C_3 ” axis. The C_3 axis of $Fm\bar{3}m$ makes the $[100]$, $[010]$, and $[001]$ directions equivalent and corresponds to superimposing the pentagons and hexagons around the hexagon perimeter, while still maintaining the hexagon centroid along the $[111]$ direction, allowing acceptable $K\cdots C$ contacts. This is shown in Figure 6 for the observed $\langle 110 \rangle$ orientation of $C_{84-D_{2d}}$.

The ability of the potassium cations to control and lock the orientation of the fulleride anions in this manner suggests

(27) Kobayashi, M.; Akahama, Y.; Kawamura, H.; Shinohara, H.; Sato, H.; Saito, Y. *Phys. Rev. B* **1993**, *48*, 16881.

(28) Fischer, J. E.; Bendele, G.; Dinnebier, R.; Stephens, P. W.; Lin, C. L.; Bykovetz, N.; Zhu, Q. *J. Phys. Chem. Solids* **1995**, *56*, 1445–1457.

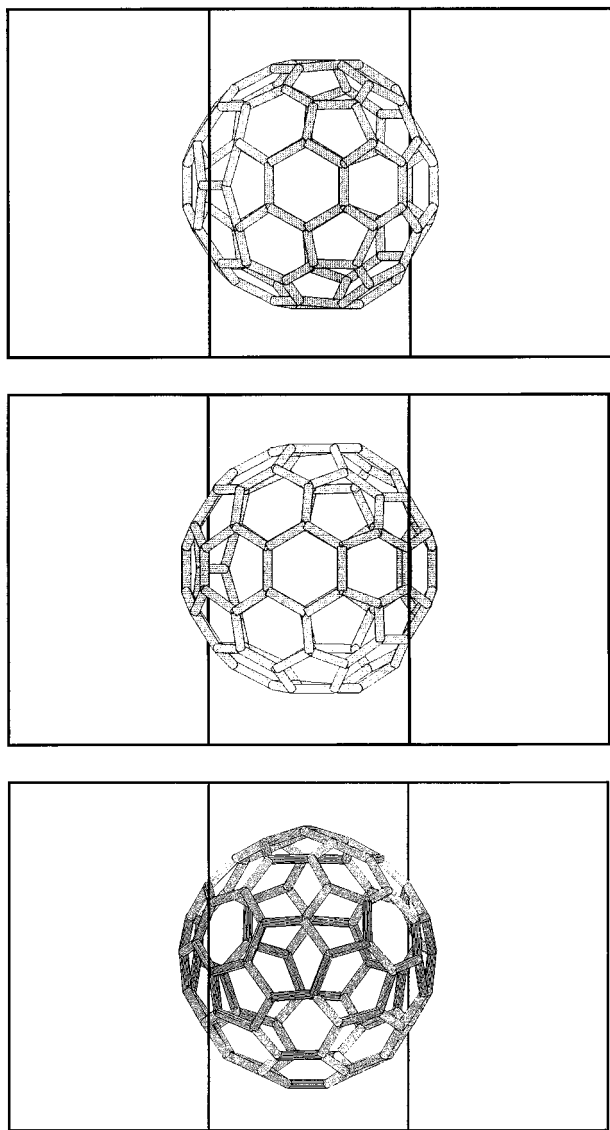


Figure 5. The preference for the $\langle 110 \rangle$ anion orientation is due to the tetrahedral cation–anion contacts. (i and ii): Views of the contacts between the tetrahedral potassium cation and two of its four closest $C_{84}\text{-}D_{2d}$ nearest neighbors in the experimentally observed $\langle 110 \rangle$ orientation, showing the alignment of the hexagon centroids along the (i) $[201]$ and (ii) $[021]$ directions. The contacts along the $[201]$ and $[021]$ directions are shown in Supporting Information. The structure is depicted in the orientationally ordered space group $I\bar{4}m2$ for clarity. The above directions in $I\bar{4}m2$ correspond to the four cube diagonal $\langle 111 \rangle$ directions in $Fm\bar{3}m$. The effect of cubic disorder on these $K\cdots C$ contacts is shown in Figure 6. (iii) The contacts between the tetrahedral potassium cation and the $C_{84}\text{-}D_{2d}$ anion viewed along the $[021]$ direction when the anion adopts the disfavored $\langle 100 \rangle$ orientation. The less favorable orientation of the six-membered ring when compared with the experimentally determined orientation shown in (i) and (ii) is clearly seen.

that it might be possible to further increase the anion orientational order using more sophisticated annealing procedures to produce more strongly tetragonal (D_{2d}) or orthorhombic (D_2) structures.

The interstitial sites in the fcc anion array are occupied (Figure 7(i)) in a manner very similar to that of the $Na_{6+x}C_{60}$ phases.^{22,23} The tetrahedral site is almost fully occupied, and there is multiple potassium occupancy of the octahedral site (Figure 7(ii)). The different refined compositions for the three phases indicate that extensive solid solution around the K_9C_{84} composition is possible. The observed scattering density on the

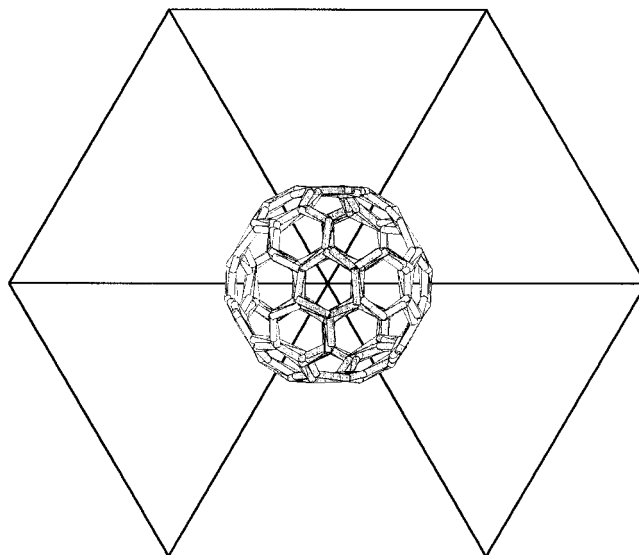


Figure 6. The orientational disorder of the $C_{84}^{9-}\text{-}D_{2d}$ anion in the observed $Fm\bar{3}m$ space group leaves the hexagon centroids aligned along the $K\cdots C$ contact vector. The $C_{84}\text{-}D_{2d}$ anion is shown in the preferred $\langle 110 \rangle$ orientation as described in the text.

octahedral site should be considered in the context of the observation of sodium cation groups with tetrahedral and cubic symmetry, which may loosely be termed clusters, on the octahedral site of the $Na_{6+x}C_{60}$ phases.^{22,23} This has generated a considerable amount of experimental activity and comparison with high-level theoretical calculations.^{29,30} Na–Na distances as short as 2.8 Å (face diagonal of an Na_4 unit in Na_6C_{60} ,²² center-corner separation of a body-centered cube in $Na_{9.7}C_{60}$ ²³) have been reported experimentally, while theory²⁹ indicates that the 2.8 Å distance may be a considerable underestimate (by up to 0.7 Å), suggesting the influence of unresolved static disorder on the refined structures. Recent ^{13}C and ^{23}Na NMR measurements indicate only partial charge transfer from the sodium grouping on the octahedral site in Na_6C_{60} .³¹ In the present $K_{8+x}C_{84}$ phases, the edge of the K_8 cube is considerably larger (3.6 Å, Table 3), consistent with the larger size of potassium.

The refined cation site occupancies (Table 2) show that approximately 25% of the octahedral site center and 75% of the cube corner sites are occupied. This suggests that these two positions are occupied in a mutually exclusive manner, that is, on 25% of the octahedral sites there are only octahedron center positions occupied and the cube corner positions are empty, whereas on the remaining 75% of the octahedral sites there are complete K_8 cubes without occupancy of the site center. This model is attractive as it removes the necessity to postulate the rather short 3.1 Å contact between the cube corner and octahedron center sites in the structure and also explains the large displacement parameter of the octahedral center cation (which would be unconstrained by the cations at the cube corners in this local picture). The smaller displacement parameters of the cube corner potassium ions also indicate that the extent of static or thermal disorder associated with the cations occupying this position is small, consistent with the close $K\cdots C$ contacts to this site. The K_8^{8+} unit deduced from these approximations is shown in Figure 8.

(29) Andreoni, W.; Giannozzi, P.; Parrinello, M. *Phys. Rev. Lett.* **1994**, *72*, 848–851.

(30) Andreoni, W.; Giannozzi, P.; Armbruster, J. F.; Fink, J. *Europhys. Lett.* **1996**, *34*, 699–704.

(31) Rachdi, F.; Hajji, L.; Galtier, M.; Yildirim, T.; Fischer, J. E.; Goze, C.; Mehring, M. *Phys. Rev. B* **1997**, *56*, 7831.

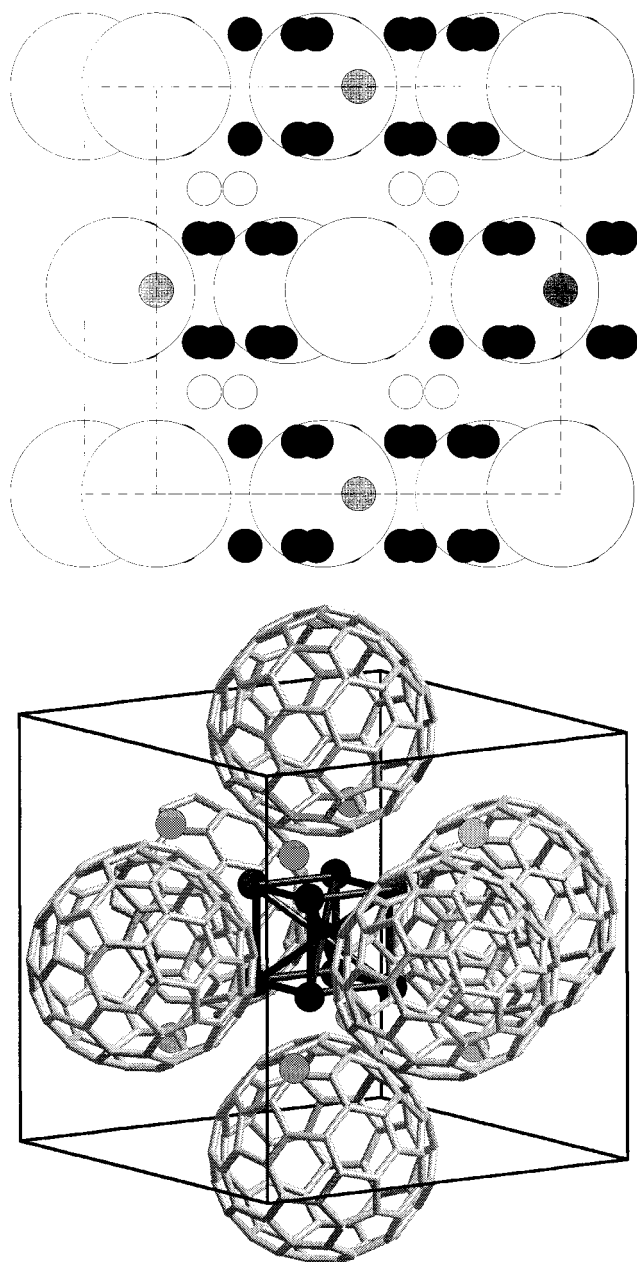


Figure 7. (i) The structure of $K_{8+x}C_{84}$ with the fulleride anions represented as unshaded spheres. Potassium cations on the octahedral site center (gray), octahedral site cube corners (black), and tetrahedral sites (light gray) are shown. (ii) One octahedral site in fcc $K_{8+x}C_{84}$, showing the potassium cations and the six surrounding $C_{84}-D_{2d}$ anions. Potassium cations occupying the tetrahedral site are shaded light gray; those on the octahedral site are black.

The dimensions of the K_8 units can be compared with the $K\cdots K$ distance in bcc potassium metal of 4.54 Å and those recently found in neutron powder diffraction refinements of potassium-loaded zeolite A of 4.2 Å.³² EPR measurements on a range of alkali metal-loaded reduced zeolites show that such cationic cluster species may act as either para- or diamagnetic traps for electrons.³³ Paramagnetic potassium clusters in zeolite cages have $g \approx 1.998$ as found for the bulk metal, seeming to indicate that in the present case the unpaired electrons are carbon-based and that the charge transfer is essentially complete.

(32) Armstrong, A. R.; Anderson, P. A.; Edwards, P. P. *J. Solid State Chem.* **1994**, *111*, 178.

(33) Woodall, L. J.; Anderson, P. A.; Armstrong, A. R.; Edwards, P. P. *J. Chem. Soc., Dalton Trans.* **1996**, 719.

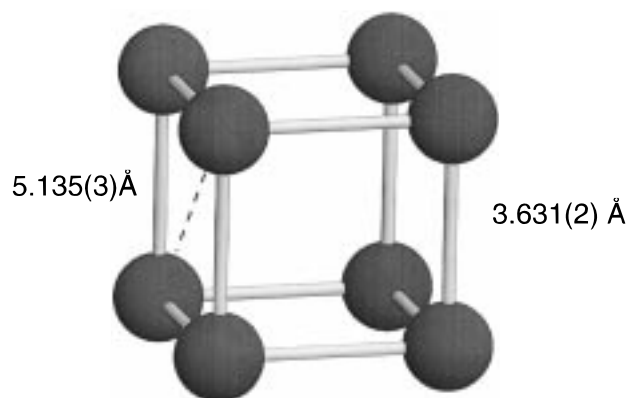


Figure 8. The K_8 cube on the octahedral site of fcc $K_{8+x}C_{84}$. The existence of this unit is deduced from the refined occupancies of the cations at the site center and cube corner positions, as discussed in the text. The distances marked are from the refinement of $K_{8.39(17)}C_{84}-D_{2d}$.

The similarities of the EPR line widths and g values to those of the C_{84}^{n-} anions found in solution³⁴ favor assignment of the observed EPR signal to the C_{84}^{n-} anions in the solid, suggesting that there is little unpaired electron density associated with the potassium cations on the octahedral site. The following discussion of the electronic structure of the C_{84} intercalates therefore treats the highest occupied states as derived purely from the fulleride anions.

EPR is the only technique to allow electronic characterization of the small available quantities of the three intercalates. The size and temperature dependence of the susceptibility (χ_{EPR}) of the mixed-isomer phase indicates that the signal measured is intrinsic, arising from localized C_{84}^{9-} anions. The EPR data thus show that mixed-isomer $K_{8.86(11)}C_{84}$ is an insulator. For a pure D_2 solid, the highest-occupied band would be close to half full at this charge. Both the LUMO and LUMO+3 of the D_{2d} isomer are doubly degenerate,³⁵ rendering the $C_{84}^{9-} D_{2d}$ anion orbitally degenerate. Single-electron band theory would thus predict the mixed-isomer C_{84}^{9-} phase to be a metal. Electron localization in this case must thus be produced by the Mott–Hubbard or polaronic mechanisms, the single-electron bandwidth being insufficient to overcome the electron–electron repulsion or electron–vibration coupling energies. It is important to bear in mind that the generally narrow bandwidths in fullerides will make the combined effects of isomer (D_2 vs D_{2d}) and orientational disorder significant in reducing the one-electron bandwidth. The observation at low temperature of distinct signals at $g = 2.00044(14)$ (D_2) and $g = 2.00047(14)$ (D_{2d}) indicates that the electronic hopping between the anions of the two isomers is slow on the EPR time scale below 40 K. This can be attributed to the existence of vibronic Franck–Condon barriers to intermolecular electron transfer between the two isomers, suggesting that polaronic effects play an important role in producing the insulating behavior.

In both the pure D_2 and D_{2d} solids, two EPR signals are observed. The interpretation of the D_2 signals as arising from noninteracting radical anions is clear from the temperature dependence of the susceptibility, but the poor agreement between the measured spin concentration and the EPR spin count suggests that at least one of the signals may be extrinsic. The number of unpaired spins in the $K_{8.39(17)}C_{84}-D_{2d}$ case is close to that expected from the refined composition; the two signals may arise from heterogeneity of the individual fulleride environ-

(34) Boulas, P.; Jones, M. T.; Kadish, K. M.; Ruoff, R. S.; Lorents, D. C.; Tse, D. S. *J. Am. Chem. Soc.* **1994**, *116*, 9393–9394.

(35) Fowler, P. W., personal communication.

ment produced by the occupancy disorder on the octahedral site. The weakly temperature-dependent signal from $K_{8.39(17)}C_{84}-D_{2d}$ is clearly intrinsic. The mixed-isomer data suggest the absence of pronounced single-ion effects in $C_{84}^{9-}-D_{2d}$ which could be responsible for the non-Curie behavior. Thus the thermal evolution of this signal indicates the presence of significant interfulleride electronic coupling for the pure D_{2d} host. The interpretation of $\chi_{EPR}(300\text{ K})$ as the Pauli susceptibility of a metallic phase yields a density of states at the Fermi level $N(E_f)$ of 1.3 states per eV per spin per C_{84} , compared with 14 states per eV per spin per C_{60} in K_3C_{60} . However, in all the $K_{8+x}C_{84}$ phases studied here, the peak-to-peak line width ΔH_{pp} is narrow and decreases on cooling. The 15 G line width from the delocalized electrons in the metallic K_3C_{60} and $(NH_3)K_3C_{60}$ ^{36,37} phases makes the metallic interpretation of the strongly interacting signal in the D_{2d} case less appealing. EPR measurements on C_{84}^{n-} ($n = 1-3$) anions of both isomers in pyridine at 120 K yielded doublet ground states (except $C_{84}^{2-}-D_{2d}$ which has a ground singlet and excited triplet state separated by 0.022 eV and D_2^{2-} which is ESR inactive) with g values between 2.002 and 2.003 and ΔH_{pp} between 1.7 and 3.9 G.³⁴ This qualitative similarity in line width of the C_{84}^{9-} solids with the isolated anions indicates that a localized electron interpretation is appropriate in this case.

Conclusion

The precise anion orientational order observed for the $K_{8+x}C_{84}$ phases and the distinct compositions and structural chemistry compared with potassium-doped C_{60} suggest that further investigation of the intercalation chemistry of C_{84} , in particular the D_{2d} isomer with its doubly degenerate LUMO, will be revealing. The structures reflect the larger interstitial sites found

(36) Allen, K. M.; Heyes, S. J.; Rosseinsky, M. J. *J. Mater. Chem.* **1996**, *6*, 1445–1447.

(37) Iwasa, Y.; Shimoda, H.; Palstra, T. T. M.; Maniwa, Y.; Zhou, O.; Mitani, T. *Phys. Rev. B* **1996**, *53*, 8836–8839.

for higher fullerenes, and the similar compositions for the two isomer-pure as well as the mixed-isomer host suggest steric/space-filling rather than electronic limitation of the number of intercalated potassium cations. The similarity in structure contrasts with the markedly different EPR properties, which depend strongly on which isomer is studied. The behavior of $K_{8.39}C_{84}-D_{2d}$ suggests that the preparation of different compositions of isomer-pure C_{84} fullerides with less than saturation doping should be a profitable undertaking.

Acknowledgment. We thank the Leverhulme Trust (M.J.R.) and Advanced Processes Research for the Future Program of JSPS (H.S.) for support of this work. K.M.A. thanks the U.K. EPSRC for a studentship and for funding a visit to Nagoya (together with the Sasakawa Fund of the University of Oxford). We thank EPSRC for access to the SRS at Daresbury Laboratory and Dr. G. Bushnell-Wye for experimental assistance on station 9.1. Dr. J. K. Cockcroft (Department of Crystallography, Birkbeck College) kindly provided his PROFIL Rietveld code including the spherical shell refinement capability. Professor P. W. Fowler (Department of Chemistry, University of Exeter) kindly provided Cartesian coordinates and Hückel molecular orbital eigenvalue spectra for both the D_2 and D_{2d} isomers of C_{84} .

Supporting Information Available: Supporting Information Available: Positions of the carbon atoms within the asymmetric unit of an fcc unit cell for both orientations of the D_2 and D_{2d} isomers of C_{84} . Views of the two orientations of the D_2 isomer. The majority EPR signal from $K_{7.91(19)}C_{84}-D_2$. The contacts between the tetrahedral cation and neighboring $C_{84}-D_{2d}$ anions along the two directions not given in Figure 5. (8 pages, print/PDF) See any current masthead page for ordering information and Web access instructions.

JA980616C